Role of membrane potential fluctuations to the criticality of neuronal avalanche activity

D E Juanico*

Rm 3111 Complex Systems Theory Group, National Institute of Physics, University of the Philippines, Diliman, Quezon City 1101, Philippines

* Corresponding author

E-mail: djuanico@gmail.com

Abstract. Experimental evidence for self-organised criticality (SOC) in non-conservative systems has recently been found in studies of rat cortical slices. The size distribution of observed neuronal avalanches has been attested to obey 3/2 power-law scaling. A mean-field sandpile model of a noisy neuronal system is proposed to refute the irreconcilability between non-conservation and criticality put forward by longstanding SOC hypotheses. The model predicts that neuronal networks achieve and maintain criticality despite non-conservation due to the presence of background activity originating from membrane potential fluctuations within individual neurons. Furthermore, small networks are demonstrated to tip towards epileptiform activity when background activity is strong. This finding ties in redundancy, an intriguing feature of brain networks, to robustness of SOC behaviour.

PACS numbers: 05.65.+b, 87.18.-h, 87.19.La

1. Introduction

One of the most recent, concrete, experimental evidence for SOC in real systems has been found in slices of rat brain tissue [1]. This new type of activity, dubbed as *neuronal avalanche*, is observed using an array of micro-electrodes placed over a neocortical slice. Neuronal avalanche has been proposed as a mode for high-speed information transmission and as a possible substrate for memory [2].

The ultimate problem with colligating this remarkable experimental phenomenon to SOC theory is the fact that information propagation between neurons via stimulus transfer is highly non-conservative [3, 4]. All SOC models so far predict that non-conservation and criticality cannot be simultaneously satisfied [5, 6, 7, 8, 9].

The goal of the present work is to demonstrate that SOC can possibly be achieved despite violation of the conservation law during stimulus transfer. In relation to this, the role of the ever-present membrane potential fluctuations as a contributory SOC mechanism in neuronal systems is explored through a mean-field model of a noisy neuronal network that exhibits avalanche activity. The findings presented here provide useful insight into how non-conservative, leaky, dissipative systems such as neuronal networks can possibly maintain a critical state in the context of SOC theory.

2. Possibility of SOC Mechanisms

A neuronal avalanche is characterised as a cascade of bursts of local field potentials (LFP), originating from synchronised action potentials triggered by the relaxation of a single neuron. When observed with a micro-electrode array, the number of electrodes that detect LFP, which is roughly proportional to the actual number of neurons synchronously firing action potentials, varies among avalanche sequences recorded at different times. The avalanche sizes are distributed approximately as an inverse power-law with exponent $\approx 3/2$. This observed trend has only so far been broadly linked with SOC principles, particularly through the study of critical branching processes [10].

Neurons receive and transmit information using one dominant form of medium—the electric potential, which is both received as input (synaptic potential) and fired as output (action potential). Each neuron stores the input as membrane potential and when this exceeds a threshold value, the neuron fires. Utilisation of a single medium in receiving, encoding, storing and transmitting information, in addition to the well-known all-or-none response of individual neurons, parallels with SOC sandpile models. A "sand grain" serves as the currency of exchange, and a sandpile site only transfers grains whenever a threshold amount of stored grains is exceeded. Thus, the critical behaviour of neuronal avalanche activity may parsimoniously, yet sufficiently, be analysed in terms of sandpile models. Furthermore, the large number of neurons ($\sim 10^{11}$ in normal human brains) and the high degree of non-local connections ($\sim 10^4$ per neuron) allow for the approximation of neuronal information transport by mean-field models.

However, prevailing SOC models are not capable of satisfying both non-conservation

and criticality. Tsuchiya and Katori offered rigorous proof that violation of the conservation law frustrates the criticality of Abelian sandpiles [5]. A mean-field treatment of the Manna sandpile known as the self-organised branching process (SOBP) by Zapperi, Lauritsen & Stanley further demonstrates that non-conservation disrupts criticality [11, 12]. Breaking of SOC due to non-conservation has also been later demonstrated numerically and analytically in the Olami-Feder-Christensen earthquake model [6, 7, 8]. The forest-fire model (FFM), which does not have conservation laws, might have been a promising SOC model, but it was ultimately proven, via Lyapunov exponent analysis [9] and later by renormalization group approach [13], that FFM is not self-organised, hence not SOC. Therefore, any attempt to subsume critical phenomena in neuronal systems within the SOC framework needs to circumvent the conceptual barricade that prevents any non-conservative system from achieving criticality.

3. Non-Conservative Mean-Field Model

3.1. Neuronal Phenomena in Sandpile Language

An individual neuron is modelled as a binary ON-OFF switch and its state z is described by mapping $\{z\} = \{0, 1, 2\}$ to its membrane potential V_{m} in relation to resting potential V_{re} and threshold potential V_{th}, as follows:

- Dormant state: $z = 0 \mapsto V_{\mathrm{re}} \leq V_{\mathrm{m}} < V_{\mathrm{th}}$
- Threshold state: $z = 1 \mapsto V_{\mathrm{m}} = V_{\mathrm{th}}$
- Excited state: $z = 2 \mapsto V_{\mathrm{m}} > V_{\mathrm{th}}$

The excited state of a neuron is highly unstable, and an excited neuron instantly de-excites by firing an action potential [14]. Hence, $z = 2$ is a transient ON state and $z = 0, 1$ are stable OFF states. This mapping concords with Manna's version of the sandpile model [15].

Grain addition and subtraction operations of the Abelian sandpile are associated with the processes known as *depolarisation* and *hyperpolarisation*, respectively. Depolarisation displaces V_{m} towards a lower value, whereas hyperpolarisation raises V_{m} to a higher value [14]. In sandpile terms, both processes can be formulated as a generic operation $z \to z + \Delta z$, where $\Delta z = +1$ for depolarisation and $\Delta z = -1$ or -2 for hyperpolarisation. An excited neuron, for instance, hyperpolarises immediately after it fires an action potential.

3.2. Neuronal Avalanche Rules

The system is a model neuronal network assumed to be fully connected and non-recurrent, i.e., each neuron links to every other neuron but not to itself. Although fully connected, a maximum of only two randomly chosen synaptic connections per neuron are activated during a single avalanche event. The network has size $N = 2^{n+1} - 1$ neurons, where n is the upper bound on the number of generations of depolarisation in

every avalanche sequence. Thus, n may be interpreted as a boundary condition, if one imagines that the neurons depolarised at the n-th generation are those situated at the network's periphery. This is in accord with the definition of boundaries for the SOBP model [11].

The entire network is in a *quiescent* state when no excited neurons are present; otherwise it is *activated*. Let us define the density of dormant and threshold neurons in a quiescent network as $1-\rho$ and ρ, respectively. The quiescent network is "slowly" stimulated via Rule A, defined as follows:

(A.1) Choose a neuron at random.

(A.2) Depolarise chosen neuron: $z \to z+1$.

If a dormant neuron is chosen at time t, Rule A is repeated in the next time step and another neuron is randomly selected. The probability that Rule A is applied to a threshold neuron at time t is $\rho = \rho(t)$. If indeed a threshold neuron is selected, it becomes excited due to Rule A.2. Consequently, time is frozen and avalanche ensues. Freezing time follows from the assumption that the ensuant avalanche event takes place instantaneously with respect to the rate at which Rule A is applied. This is what is essentially meant by "slow" stimulation, conventionally referred to as "infinite time-scale separation," which is justified by the fact that the time interval between two distinct avalanche sequences is much longer than the duration of a single avalanche sequence [1]. Infinite time-scale separation is also a typical assumption in sandpile models [16].

The ensuant events following the emergence of an excited neuron are collectively referred to as Rule B:

(B.1) Randomly choose two post-synaptic neurons (u and v) connected to excited neuron w.

(B.2) After firing an action potential, w immediately hyperpolarises, and u and v may depolarise. Three cases possible:

  (a) With probability α, w hyperpolarises to dormant state ($z_w : 2 \to 0$); both u and v depolarise.

  (b) With probability β, w hyperpolarises back to threshold state ($z_w : 2 \to 1$); only one of either u or v depolarises.

  (c) With probability $\epsilon = 1-\alpha-\beta$, w hyperpolarises to dormant state ($z_w : 2 \to 0$); neither u nor v depolarise.

(B.3) Repeat B.1 and B.2 until all excited neurons are depleted, or after n generations of depolarisation are reached.

(B.4) Resume Rule A.

Rule B essentially describes the avalanche sequence, which only terminates if the activated network relaxes back to its quiescent state (i.e., no excited neurons present), or after the boundary condition (i.e., n generations of depolarisation) is met. Time takes off again after Rule B terminates and once more the network builds up for the

next avalanche event via Rule A. The total number of neurons s depolarised during the sequence is defined as the *avalanche size*.

3.3. Background Activity

The significant distinction of this model from typical sandpile models is the presence of *background activity*—the system is a *noisy* neuronal network. This is conceived by postulating the existence of membrane potential fluctuations inside each individual neuron when the network is quiescent. This postulate is motivated by electrophysiological studies on membrane potential transitions that arise through activation of a *hyperpolarisation-activated cation current* or H-current [17]. Kang, Kitano & Fukai have demonstrated that membrane potential fluctuations "can be generated through a spike-timing-dependent self-organizing process in a network of inhibitory neurons and excitatory neurons expressing the H-current," using a realistic model of a cortical neural network [17]. Spike-timing dependent processes that affect the probability with which a neuron fires an action potential have also been investigated experimentally in whole-cell recordings of cortico-striatal slices [18]. The existence of membrane potential fluctuations is also linked to the presence of background noise in neuronal activity, which has been found to play a significant role in neuronal responsiveness to varying intensities of stimuli (see [19] for a review). The role of background noise is analogous to *stochastic resonance*, a well-studied nonlinear phenomenon with a wealth of following in the neuroscience and computational neuroscience research community [20, 21, 22, 23, 24].

The level of background activity in the quiescent network is quantified by a parameter $\eta \in (0, 1]$. The background activity is denoted as Rule C, defined as follows:

(C.1) With probability η, a dormant neuron depolarises to threshold state ($z : 0 \to 1$).

(C.2) With probability $\eta(\sigma/\rho - 1)$, a threshold neuron hyperpolarises to dormant state ($z : 1 \to 0$),

where σ is known as the *branching parameter*, to be discussed in more detail in section 4. At time t, Rule C is concurrent with Rule A and operates over the entire network in parallel. It changes $\rho(t)$ for the next time step $t + \Delta t$ such that Rule C.1 contributes, on the average, a change to ρ

$$\rho(t + \Delta t) - \rho(t) = \eta[1 - \rho(t)]\Delta t\,, \tag{1}$$

and Rule C.2 contributes

$$\rho(t + \Delta t) - \rho(t) = -\eta \left[\frac{\sigma(\rho(t))}{\rho(t)} - 1\right] \rho(t)\Delta t\,, \tag{2}$$

where σ/ρ is the local branching parameter. Since Rules C.1 and C.2 happen concurrently, then (1) and (2) can directly be added together to yield a net change in ρ per unit time

$$\mathcal{B}(\rho; \eta) = \eta\,[1 - \sigma(\rho)]\ . \tag{3}$$

Table 1. Transition rules of the non-conservative mean-field model with corresponding transition probabilities. The central digits for the avalanche rules correspond to the excited agent and the flanking digits are the two random neighbors, in no particular order. The sum of transition probabilities for the avalanche and nonconservative rules is ρ, which is, self-consistently, the probability that the avalanche had initiated.

Process	Rule	Transition probability
Background activity	$1 \to 0$	$\eta(\sigma/\rho - 1)\rho$
	$0 \to 1$	$\eta(1-\rho)$
Avalanche	$121 \to 202$	$\alpha\rho^3$
	$021 \to 102$	$2\alpha\rho^2(1-\rho)$
	$020 \to 101$	$\alpha\rho(1-\rho)^2$
	$121 \to 112$	$\beta\rho^3$
	$021 \to 012$	$2\beta\rho^2(1-\rho)$
	$020 \to 011$	$\beta\rho(1-\rho)^2$
Non-conservation	$2 \to 0$	$\epsilon\rho = (1-\alpha-\beta)\rho$

Equation (3) serves as the phenomenological model of background activity. $\mathcal{B}$ is excitatory (i.e., increases ρ) when $\sigma < 1$, and inhibitory (i.e., decreases ρ) when $\sigma > 1$. Experimental evidence suggests that this seesaw between cortical excitation and inhibition contributes in stabilising the network, keeping it on the border between inactivity and epileptiform activity [4].

4. Dynamics and Branching Process

The transition rules of the model are summarised in table 1. Background activity is derived from Rule C. The first three avalanche rules are from Rule B.2.a, whereas the last three are from Rule B.2.b. The non-conservation process is taken from Rule B.2.c, so that ϵ measures the level of non-conservation of the model. Conservation law is essentially violated when $\epsilon > 0$.

Given the transition rules, the density ρ, assumed to be a continuous dynamical variable, satisfies

$$\frac{\mathrm{d}\rho}{\mathrm{d}t} = \mathcal{B}(\rho;\eta) + \mathcal{A}(\rho;\epsilon) + \chi(t)\,. \tag{4}$$

The noise term $\chi(t)$ arises from the probabilistic nature of the transition rules, and accounts for the fluctuations around average values assumed to hold in the mean-field calculations. It appropriately vanishes in the large-N limit, which has been confirmed through numerical simulations. The term $\mathcal{A}(\rho;\epsilon)$ represents the change in $\rho(t)$ due to depolarisations brought about by an avalanche at time t. Treating the avalanche as a branching process, and following closely the analysis in [12], $\mathcal{A}(\rho;\epsilon)$ satisfies

$$N\mathcal{A} = 1 - \sigma^n - \frac{\epsilon\rho}{1-(1-\epsilon)\rho}\left[1 + \frac{1-\sigma^{n+1}}{1-\sigma} - 2\sigma^n\right], \tag{5}$$

where the first term comes from Rule A acting on a threshold neuron with probability $\rho(t)$ at time t. The second term represents the average amount of stimuli dissipated by threshold neurons becoming excited in the n-th generation. The third term, which is non-zero when $\epsilon > 0$, represents the average amount of stimuli lost due to transmission failure (non-conservation [Rule B.2.c]). The branching parameter σ is derived from the following definition

$$\sigma = \sum_k kq(k)\,, \tag{6}$$

wherein from table 1, the branching probability $q(k)$ that an excited neuron subsequently depolarises k other neurons is

$$q(k) = \alpha\rho\delta_{k,2} + \beta\rho\delta_{k,1} + [1 - (1-\epsilon)\rho]\,\delta_{k,0}\,, \tag{7}$$

with $\delta_{i,j}$ being the Kronecker delta. The first and second terms in (7) are the sum of transition probabilities of the first three avalanche rules and of the last three avalanche rules listed in table 1, respectively. The last term is the total of the probability coming from the non-conservation rule and the probability that a dormant neuron is depolarised, which both yield $k = 0$. Substitution of (7) to (6) renders

$$\sigma = (2\alpha + \beta)\rho\,, \tag{8}$$

which depends on α and β, and is proportional to density ρ. In this model it is assumed that α and β remain fixed throughout so that the only dynamic variable is ρ. Consequently,

$$\frac{\mathrm{d}\sigma}{\mathrm{d}t} = (2\alpha + \beta)\frac{\mathrm{d}\rho}{\mathrm{d}t}\,. \tag{9}$$

A branching process is sub-critical when $\sigma < 1$, for which avalanches have sizes no larger than a finite cutoff size no matter how large the system is. On the other hand, a branching process is supra-critical when $\sigma > 1$ such that avalanches as large as the system itself are formed almost with certainty. Hence, $\sigma = 1$ is a critical value that results to a critical branching process [25]. The avalanche size distribution emerging from a critical branching process is expected to be power law. Since σ only varies when ρ changes, then ρ determines whether the branching process is sub-critical, critical, or supra-critical.

5. Avalanche Size Distribution

A diagram of an avalanche is illustrated as a binary branching tree in figure 1. The initial excited neuron emerging from Rule A at time t with probability $\rho(t)$ is the topmost node. During the avalanche, it depolarises two neurons with probability $\alpha\rho$, both becoming excited. One of these depolarises one neuron with probability $\beta\rho$. Also shown is an excited neuron that does not depolarise any neuron with probability $\epsilon\rho$ due to non-conservation. Setting $n = 3$, all excited neurons at three levels below the topmost node do not further depolarise other neurons. In the example shown, the avalanche size is $s = 9$.

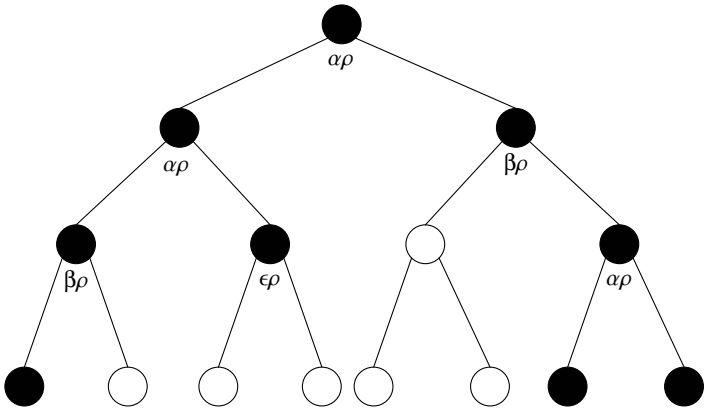

Figure 1. Avalanche shown as a branching tree with $n = 3$. Shaded circles corresponded to depolarised neurons. The avalanche size $s = 9$ corresponds to the total number of shaded circles.

The branching probability $q(k)$ defined in (7) fundamentally describes the likelihood that an excited neuron subsequently depolarises $k \in \{0, 1, 2\}$ neurons in the succeeding generation. With $q(k)$ the avalanche size distribution $P(s)$ is calculated using a generating functional formalism. A generating function $\mathcal{F}_m(\omega)$ of $P(s)$ after m generations is defined as

$$\mathcal{F}_m(\omega) = \sum_{s=1}^{\infty} P(s)\omega^s \,. \tag{10}$$

$\mathcal{F}_m$ is also considered the m-th iterate of the generating function $\mathcal{F}_1 := \mathcal{F}$

$$\mathcal{F}(\omega) = \sum_{s=1}^{\infty} q(s-1)\omega^s = \omega \sum_{s=1}^{\infty} q(s-1)\omega^{s-1} \,. \tag{11}$$

Furthermore, by definition $\mathcal{F}_{m+1}(\omega) = \mathcal{F}[\mathcal{F}(\omega)]$, such that from (11), the following sufficiently holds [25]

$$\mathcal{F}_{m+1}(\omega) = \omega \sum_{s=1}^{\infty} q(s-1) \left[\mathcal{F}_m(\omega)\right]^{s-1} \,, \tag{12}$$

which simplifies to

$$\mathcal{F}_{m+1}(\omega) = \omega \left\{ \alpha\rho\mathcal{F}_m^2 + \beta\rho\mathcal{F}_m + [1 - (1-\epsilon)\rho] \right\} \,, \tag{13}$$

following from (7). For sufficiently large m, the theory of branching processes asserts a self-consistency relation wherein $\mathcal{F}_{m+1} \simeq \mathcal{F}_m$, so that solving for $\mathcal{F}_m$ in (13) yields

$$\mathcal{F}_m(\omega) = \frac{1 - b\omega - \sqrt{1 - 2b\omega + a\omega^2}}{2\alpha\rho\omega} \,, \tag{14}$$

where $a = \beta^2\rho^2 - 4\alpha\rho[1 - (1-\epsilon)\rho]$, and $b = \beta\rho$. Binomial expansion of (14) around its singularity $\omega = 0$ yields a power series of the form defined in (10). The coefficients of expansion correspond to $P(s)$. In a more compact form the solution can be expressed as a recurrence relation

$$P(s) = \frac{1}{s+1} \left[(2s-1)bP(s-1) - (s-2)aP(s-2) \right] \,. \tag{15}$$

In particular, Pinho & Prado [7] have calculated an analytic form of (15) for the special case of $\beta = 0$. Equation (15) can easily be demonstrated, by graphical inspection, to have the asymptotic behavior $P(s) \sim s^{-3/2}$ for $s \gg 1$ if $a = 2b - 1$; a condition that can equivalently be expressed as

$$\begin{aligned} Q(\rho) &= a - 2b + 1 \\ &= \beta^2\rho^2 - 4\alpha\rho[1 - (1 - \epsilon)\rho] - 2\beta\rho + 1 \\ &= 0\,. \end{aligned} \tag{16}$$

Since $\sigma \propto \rho$ from (8), then (16) can also be expressed as $Q(\sigma)$ with root at $\sigma = 1$, which is the critical value of the branching parameter.

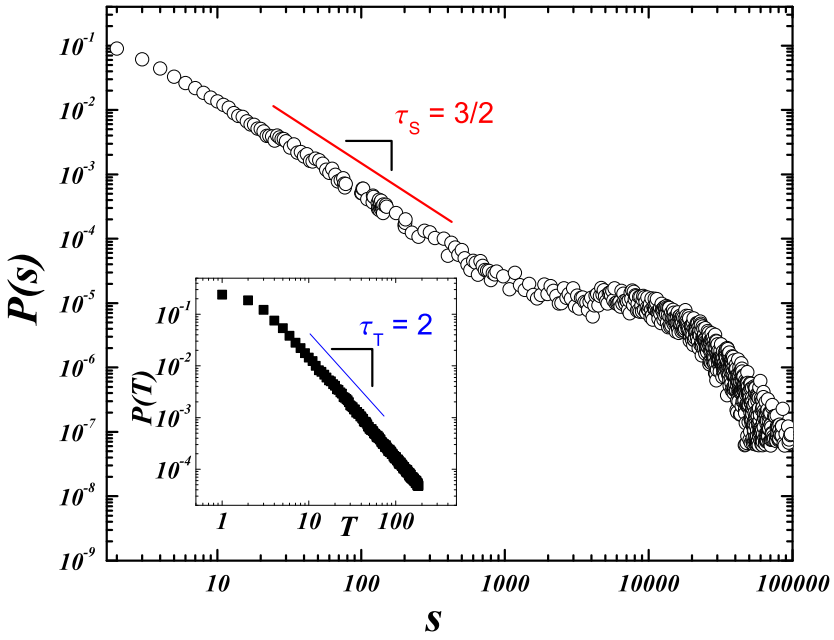

Figure 2. Typical avalanche size distribution from simulation of the model with $\epsilon = 0.2$, $\eta = 0.03125$ and $n = 183$. $P(s)$ exhibits power-law scaling with exponent 3/2 spanning three orders of magnitude. The fat tail is an artifact of finite n, which moves to the right by simply increasing n. The inset graph is the distribution of avalanche lifetime T, which is the actual number ($\leq n$) of generations of depolarisations before the avalanche dies out. A power-law with exponent 2 is drawn as guide.

Numerical simulations of the model also confirms the asymptotic behavior of $P(s)$, as shown in figure 2. Note that by increasing n, the scaling trend also extends to the right so that the power-law regime also spans a wider range of orders, as expected for a truly critical system. In figure 2, the 3/2-scaling in $P(s)$ extends roughly three orders of magnitude. Also shown is the avalanche lifetime distribution $P(T)$, which also exhibits scaling with exponent 2.

6. Results and Discussion

The stationary behaviour of the model is examined using a well-established geometrical theory of fixed points [26]. Nonlinear differential equations such as (9) may be analysed graphically in terms of vector fields. In this framework, $\dot{\sigma} := \mathrm{d}\sigma/\mathrm{d}t$ is interpreted as a "velocity vector" at each possible σ value. A plot of $\dot{\sigma}$ versus σ is known as the phase portrait of the model. The fixed point σ^* corresponds to the σ-value at which $\dot{\sigma} = 0$. The trajectory of the vector around the neighbourhood of this fixed point is directed to the right where $\dot{\sigma} > 0$, and to the left where $\dot{\sigma} < 0$. This means that if $\dot{\sigma}$ is increasing around the neighbourhood of σ^*, then the fixed point is repulsive. On the other hand, if $\dot{\sigma}$ is decreasing, then the fixed point is attractive.

Linearisation of (9) actually yields

$$\lim_{\sigma\to\sigma^*} \frac{\partial}{\partial\sigma}\frac{\mathrm{d}\sigma}{\mathrm{d}t} < 0\,,$$

which implies that the fixed points of the model are attractive. This is confirmed by plotting the actual phase portraits for different n, shown in figure 3. The plots are monotonically decreasing, implying that indeed the fixed points of (9) are dynamically attractive. Therefore, the network spontaneously approaches (without the tuning of control parameters) the state defined by its fixed point—the essence of self-organisation.

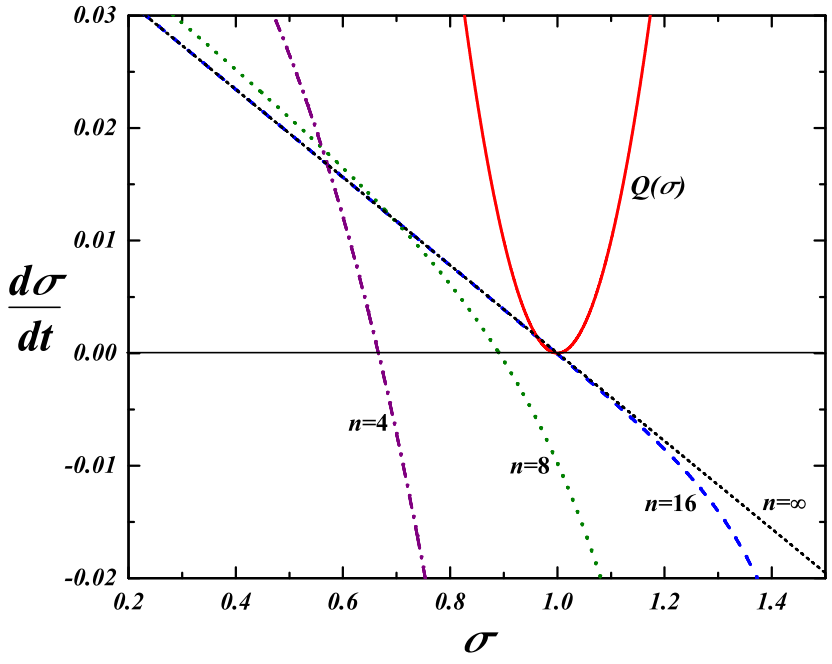

Figure 3. Phase portrait, showing $\dot{\sigma}$ versus σ, for a non-conservative system with $\epsilon = 0.25$ and $\eta = 0.03125$ of different sizes $N = 2^{n+1} - 1$: 31 (chain curve), 511 (dotted curve), 131,071 (dashed curve), and ∞ (broken line). The fixed points σ^* correspond to the root of $\dot{\sigma}$. The solid parabola is the function $Q(\sigma)$ with root at $\sigma = 1$. For $N \geq 131,071$, $\sigma^* = 1$, indicating that the non-conservative system spontaneously evolves towards its critical state via self-organisation.

Also illustrated in figure 3 is the parabolic function $Q(\sigma)$ with a root at $\sigma = 1$. For network sizes $N = 31$ and $N = 511$, obviously $\sigma^* < 1$, implying that the network self-organises towards a sub-critical state. However, from $N = 131,071$ up to $N \to \infty$, $|1 - \sigma^*| \ll 1$. A non-conservative network achieves SOC even if its size is finite. The rapid approach of σ^* towards 1 from $N = 511$ to $N = 131,071$ in addition to the decelerating change in σ^* from $N = 131,071$ to $N \to \infty$ indicates a phase transition.

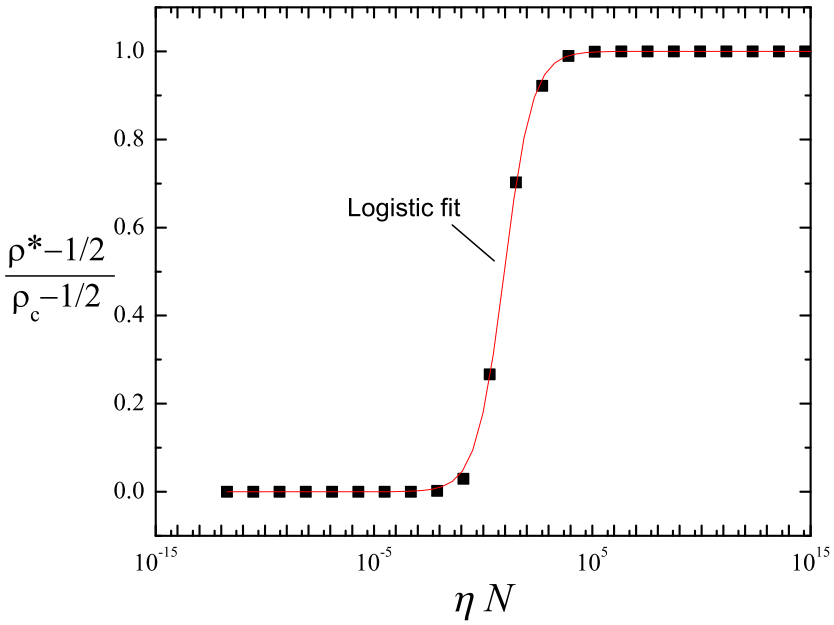

Figure 4. Phase transition in the non-conservative model. Data points result from numerical analysis of the fixed point density ρ^* of (4) neglecting the noise term $\chi(t)$, for various $\epsilon \in (0, 1/2)$, $\eta \in (0, 1]$, and system size N. The critical density $\rho_c = (2\alpha + \beta)^{-1}$ is derived from (8) with $\sigma = 1$. The curve is a logistic fit of the form $y(x) = 1 - [1 + (x/\theta)^\gamma]^{-1}$ where $y = (\rho^* - 1/2)/(\rho_c - 1/2)$ and $x = \eta N$.

Indeed as shown in figure 4, the model reveals a phase transition. The data points are derived from numerical fixed-point analysis of (4), assuming that the noise term $\chi(t)$ is very small to be significant. For a wide range of non-conservation levels $\epsilon \in (0, 1/2)$, and background activity $\eta \in (0, 1]$, a phase diagram emerges from the relation between $(\rho^* - 1/2)/(\rho_c - 1/2)$ and ηN. The resultant plot is fitted by a logistic curve

$$\frac{\rho^* - 1/2}{\rho_c - 1/2} = 1 - \left[1 + \left(\frac{\eta N}{\theta}\right)^\gamma\right]^{-1}, \tag{17}$$

wherein ρ^* is the steady-state density corresponding to the fixed-point branching parameter σ^*, and ρ_c is the critical density derived from (8) with $\sigma = 1$. The fitting parameters are $\theta = 9.31 \pm 0.27$ and $\gamma = 0.68 \pm 0.01$ (goodness of fit: $\chi^2/\mathrm{DoF} = 4 \times 10^{-5}$, $R^2 = 0.99986$, no weighting). Equation (17) suitably describes two limiting cases of the model. The first one is $\eta \to 0$, which results to $\rho^* \to 1/2$. This limiting case is equivalent to having no background activity, as in the SOBP model by Lauritsen, Zapperi & Stanley [12]. They have similarly found that the steady-state density $\rho^* = 1/2$,

irrespective of any level of non-conservation ϵ. Consequently, the SOBP model is always sub-critical (i.e., yields no power-law but rather exponentially truncated distributions) whenever $\epsilon > 0$. Therefore, a neuronal network without background activity in the form of membrane potential fluctuations cannot display SOC.

The second limiting case corresponds to $\eta N \gg \theta$, which leads to $\rho^* \to \rho_c$. At this limit, the non-conservative system is always critical. A closer look at figure 4 reveals that the data points lie infinitesimally close to 1 starting at $\eta N \sim 10^4$. This means that if the network is very large, say $N \sim 10^{11}$ which is typical of normal human brain networks, then for a very wide range of background activity $\eta \in (10^{-7}, 1]$, the non-conservative network is always expected to exhibit SOC behaviour in the form of neuronal avalanche activity. Simulation of the model for various levels of non-conservation ϵ likewise yields an avalanche size distribution $P(s)$ of the form plotted in figure 2.

It is also interesting to note that for $\eta N \simeq \theta$, the fixed-point density ρ^* is highly uncertain to small variations in either η or N. This is the regime describing the abrupt rise from 0 to 1 in figure 4.

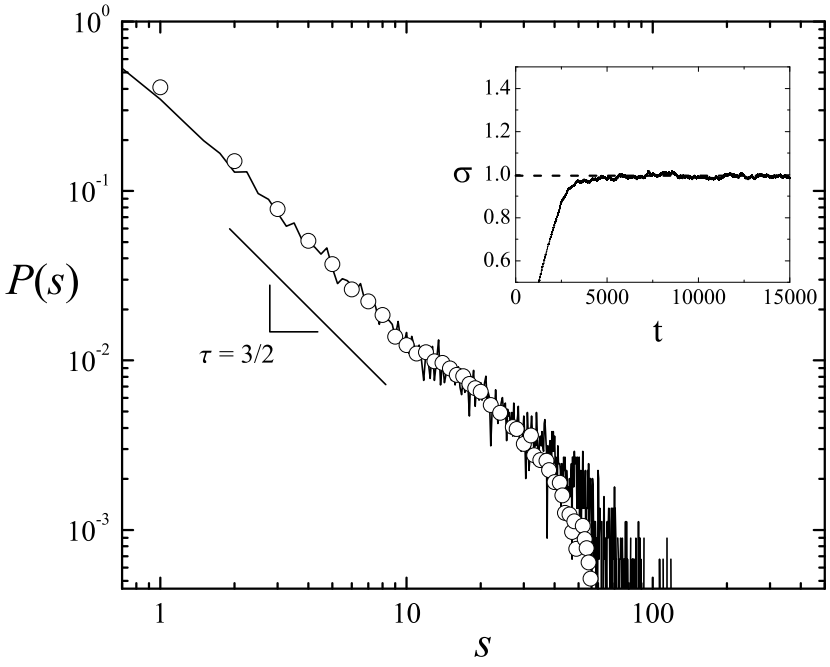

Figure 5. Distribution of neuronal avalanche size data adopted from [10] (circles), and of a simulated network (full curve) with $\eta N \approx 3,670$ having a level of non-conservation $\epsilon = 0.25$. Inset graph shows $\sigma(t)$ as a function of time t, approaching the critical value of 1 at the steady-state.

A simulation of the model is performed for a network with size $N = 131,071$ with background activity $\eta = 0.025$ such that $\eta N \approx 3,670$, and level of non-conservation $\epsilon = 0.25$. After rescaling the simulated avalanche sizes with a factor deduced from experiment [1], the model successfully fits the neuronal avalanche size distribution $P(s)$ adopted from [10], as shown in figure 5. A power-law with exponent 3/2 primarily characterises the distribution, as predicted. A cutoff appears because of

the limited number of micro-electrodes utilised in resolving LFP intensity during the experiments [1]. The cutoff shifts to the right (i.e., towards larger avalanche sizes) when the number of micro-electrodes is increased. Data from simulation also fits this cutoff remarkably well. The cutoff in the simulation arises from the imposed boundary condition limiting the number of generations of depolarisation in a single avalanche. This cutoff also shifts to the right by increasing n. Hence, both model and experimental data agree not only in the power-law behaviour of $P(s)$, but also with regards to the underlying cause of the cutoff. The inset graph illustrates the evolution of the branching parameter σ with time t, approaching the critical value of 1 at the steady state. This

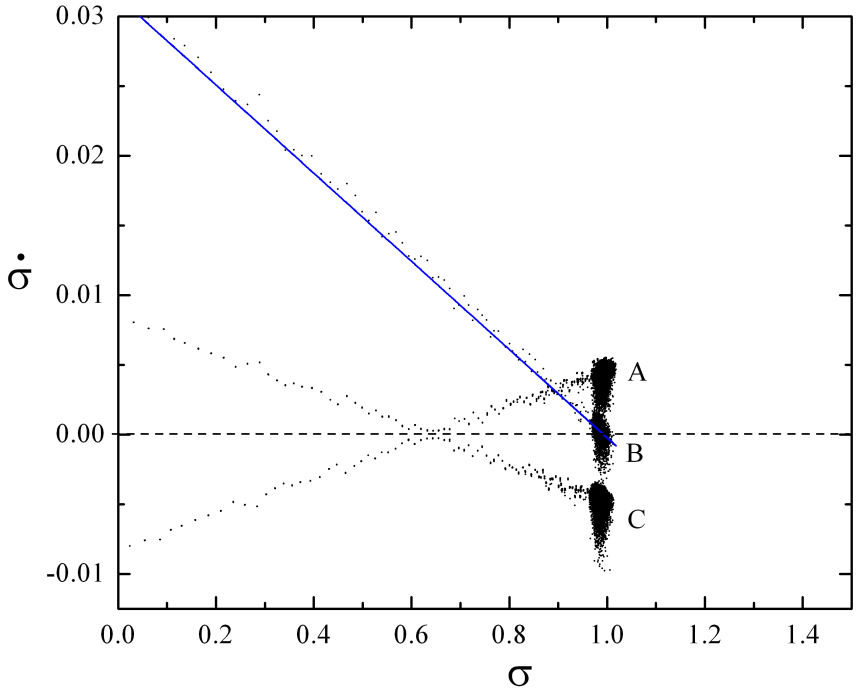

Figure 6. Phase plot of the simulated network converging towards three dynamical attractors: (A) excitatory membrane potential fluctuations; (B) fixed point ($\sigma^* = 1$); and (C) inhibitory membrane potential fluctuations. Solid line is the phase portrait based on numerical analysis of (9), neglecting noise $\chi(t)$.

steady-state behaviour is supported by a phase plot of σ, shown in figure 6. The fixed point (B) corresponds to $\sigma^* = 1$. Also shown are two other dynamical attractors (A, C), which correspond to the noise $\chi(t)$ that was neglected in the fixed-point analysis of (9). The symmetry between (A) and (C) indicates a balance between cortical excitation and inhibition, which consequently imparts stability to the network's critical steady-state (i.e., σ remains sufficiently close to 1 at any time). Thus, the background activity due to membrane potential fluctuations is essential in letting the network hover around the critical state such that a power-law $P(s)$ is generated.

High redundancy has been regarded as one of the most intriguing characteristics of the human brain. The presence of several identical neurons that perform similar roles may be colligated with robust performance. Robustness of the network's

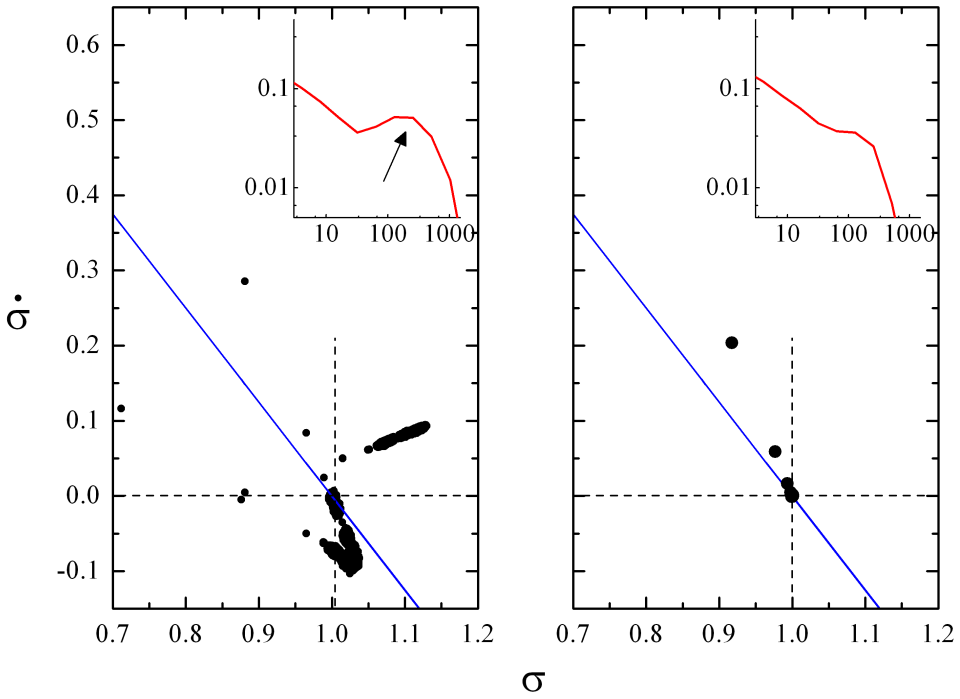

Figure 7. Phase plots for two simulated networks of different sizes N but similar levels of non-conservation $\epsilon = 0.25$ driven by a strong background $\eta = 1.0$. Expected fixed point is at $\sigma^* = 1$. *Left panel.*— $N = 131,071$ neurons, showing a prominent excursion at a region where $\sigma > 1$ and $\dot{\sigma} > 0$. Solid line corresponds to mean-field prediction neglecting noise $\chi(t)$. Inset graph displays the resultant logarithmically-binned histogram of avalanche sizes, having a marked peak (pointed by arrow) for large sizes, suggestive of *epileptiform activity*. *Right panel.*— $N = 4,194,303$ neurons, exhibiting fixed-point stability at $\sigma^* = 1$. Inset graph presents the logarithmically-binned $P(s)$.

critical behaviour with respect to background intensity is examined by comparing the performance of a small ($N = 131,071$) and a large ($N = 4,194,303$) network driven by a strong background ($\eta = 1.0$).

Figure 7 (*Left panel*) shows the phase plot of the small network exhibiting imbalance in the excitatory and inhibitory dynamical attractors. There is a notable excursion of the phase plot on a region wherein $\sigma > 1$ and $\dot{\sigma} > 0$. This implies that the network is highly excited—i.e., more frequently, a majority of neurons are synchronously firing action potentials. The inset graph reveals a high occurrence probability of large neuronal avalanches as implied by the presence of a hump. High degree of synchronisation has been believed to be the precursor of epileptic seizure attacks [14]. Epilepsy is also oftentimes attributed to damage of nerve cells resulting from accidents or neuro-degenerative diseases thereby cutting down the network's redundancy, hence its robustness to over-excitation.

On the other hand, figure 7 (*Right panel*) shows that the large network is highly robust even to a strong background intensity. This supports the link between redundancy and robustness. The inset graph of the avalanche size distribution does not

exhibit a hump. The large network therefore maintains its critical behaviour despite the intensiveness of membrane potential fluctuations.

7. Possible Extension of the Model

The model's effectiveness relies on having the branching parameter defined in (8) spontaneously converge to the critical value of 1. A key assumption is that α and β are fixed, so that $\sigma = 1$ is achieved solely by means of the background activity. One could assume instead that both α and β, which both represent *synaptic efficacy*, also change in time. Efficacy of synaptic transmission changes as a result of *synaptic plasticity*—the dynamical adjustment of the strength of connections between neurons [14]. This assumption consequently yields the generalisation (9)

$$\frac{\mathrm{d}\sigma}{\mathrm{d}t} = \left(2\frac{\partial\alpha}{\partial t} + \frac{\partial\beta}{\partial t}\right)\rho + (2\alpha + \beta)\,\frac{\partial\rho}{\partial t}\,.$$

The implementation of the above modification incorporates the role of synaptic plasticity to the criticality of neuronal avalanche activity.

8. Summary and Conclusion

Recent experimental evidence for SOC discovered in neuronal networks has primarily motivated this research. A non-conservative mean-field sandpile model of SOC has been proposed to address the irreconcilability between critical behaviour manifested by the power-law size distribution of neuronal avalanches and the inherent non-conservation of information transmission of neuronal networks in the context of prevailing SOC theory and models. Critical behaviour has been analysed in terms of the theory of branching processes and fixed-point methods. Consequently, it generates scale-invariant avalanche size distributions as demonstrated by theoretical analysis and numerical simulations. The findings provide useful insight into the possible role of membrane potential fluctuations, which effectively generates background activity, on how dissipative neuronal networks maintain a critical state despite non-conservation. Furthermore, the model has been able to associate network redundancy, which is an intriguing characteristic of brain networks, to network robustness. Small networks which are relatively less redundant than large networks may tip towards epileptiform activity when membrane potential fluctuations are strong.

References

[1] Beggs J M and Plenz D 2003 *J. Neurosci.* **23** 11167
[2] Beggs J M and Plenz D 2004 *J. Neurosci.* **24** 5216
[3] Vogels T P and Abbott L F 2005 *J. Neurosci.* **25** 10786
[4] Galarreta M and Hestrin S 1998 *Nature Neurosci.* **1** 587
[5] Tsuchiya T and Katori M 2000 *Phys. Rev.* E **61** 1183
[6] Drossel B 2002 *Phys. Rev. Lett.* **89** 238701

[7] Pinho STR and Prado CPC 2003 *Braz. J. Phys.* **33** 476
[8] Boulter C J and Miller G 2003 *Phys. Rev.* E **68** 056108
[9] Socola J E S, Grinstein G and Jayaprakash C 1993 *Phys. Rev.* E **47** 2366
[10] Haldeman C and Beggs J M 2005 *Phys. Rev. Lett.* **94** 058101
[11] Zapperi S, Lauritsen K B and Stanley H E 1995 *Phys. Rev. Lett.* **75** 10786: 4071
[12] Lauritsen K B, Zapperi S and Stanley H E 1996 *Phys. Rev.* E **54** 2483
[13] Loreto V, Pietronero L, Vespignani A and Zapperi S 1995 *Phys. Rev. Lett.* **75** 465
[14] Purves D *et al* , eds. 2004 *Neuroscience, Third ed.* (Sunderland, MA: Sinauer Associates)
[15] Manna S S 1991 *J. Phys. A: Math. Gen.* **24** L363
[16] Vespignani A and Zapperi S 1998 *Phys. Rev.* E **57** 6345
[17] Kang S, Kitano K and Fukai T 2004 *Neural Networks* **17** 307
[18] Mahon S, Cassasus G, Mulle C and Charpier S 2003 *J. Physiol.* **550** 947
[19] Destexhe A and Conteras D 2006 *Science* **314** 85
[20] Meunier C and Segev I, in Moss F and Gielen S, eds. 2000 *Handbook of Biological Physics* **4** 426 (Amsterdam: Elsevier)
[21] Kish L B, Harmer G P and Abbott D 2001 *Fluct. Noise Lett.* **1** L13
[22] Longtin A 2002 *Fluct. Noise Lett.* **2** L183
[23] Ginzburg S L and Pustovoit M A 2003 *Fluct. Noise Lett.* **3** L265
[24] Arecchi F T 2005 *Fluct. Noise Lett.* **5** L163
[25] Harris T E 1963 *The Theory of Branching Processes* (Berlin: Springer-Verlag)
[26] Strogatz S H 1994 *Nonlinear Dynamics and Chaos: With Applications to Physics, Biology, Chemistry, and Engineering* (Reading, MA: Perseus Books)